Available online at www.sciencedirect.com
ScienceDirect
Journal of Molecular Graphics and Modelling 27 (2008) 13–19
Journal of Molecular Graphics and Modelling
www.elsevier.com/locate/JMGM

Nanosecond molecular dynamics simulations of Cdc25B and its complex with a 1,4-naphthoquinone inhibitor: Implications for rational inhibitor design

Sungmin Ko [a,1], Woojin Lee [b,1], Sangyoub Lee [b,**], Hwangseo Park [a,*]

[a] Department of Bioscience and Biotechnology, Sejong University, 98 Kunja-Dong, Kwangjin-Ku, Seoul 143-747, Republic of Korea
[b] Department of Chemistry, Seoul National University, Seoul 151-747, Republic of Korea

Received 29 October 2007; received in revised form 28 January 2008; accepted 5 February 2008
Available online 16 February 2008

Abstract

Cdc25 phosphatases have been considered as attractive drug targets for anticancer therapies due to the correlation of their overexpression with a wide variety of cancers. To gain insight into designing new potent inhibitors, we investigate the dynamic properties of Cdc25B and its complex with a 1,4-naphtoquinone inhibitor NSC 95397 by means of molecular dynamics simulations in aqueous solution. It is shown from the calculated dynamic properties that the malleability of the residues 530–532 residing at the start of C-terminal region around the active site should be responsible for the catalytic action of Cdc25B. However, binding of the inhibitor in the active site leads to a substantial decrease in the motional amplitude of the flexible residues, due to the hydrophobic interactions with the side chain of Met531. The simulation results also indicate that at least four hydrogen bonds are involved in the enzyme-inhibitor complex. Among them, the hydrogen bond between the side chain carboxylate group of Glu478 and one of the hydroxyl groups of the inhibitor is found to be the most significant binding force stabilizing the inhibitor in the active site. This result supports the previous experimental implication that the possession of a single hydroxyl group is sufficient for the inhibitory activity of 1,4-naphthoquinone inhibitors.

Keywords: Cdc25B; Inhibitor; Molecular dynamics; Docking; Hydrogen bond

1. Introduction

Cdc25 phosphatases belong to a class of dual-specificity phosphatases that are responsible for dephosphorylating both threonine and tyrosine side chains of a protein substrate. Of the three Cdc25 homologues (Cdc25A, Cdc25B, and Cdc25C) encoded in human genome, Cdc25A and Cdc25B are shown to have oncogenic properties [1]. Cdc25A participates in the control of the transitions in cell cycle from Gap 1 (G_1) to synthesis (S) phases and from Gap 2 (G_2) to mitosis (M) phases by dephosphorylating and activating cyclin-dependent kinase (Cdk)/cyclin complexes, while Cdc25B is mainly involved in regulating the progression at the G_2-to-M transition [2]. Thus, Cdc25 phosphatases play a significant role in the regulation of the eukaryotic cell cycle progression by activating the Cdk/cyclins that serve as the central regulators of the cell cycle with the role of driving each state of cell division.

Due to such an important contribution to the cell cycle regulation, Cdc25 phosphatases have been considered to be involved in oncogenic transformations and human cancers. The overexpression of Cdc25A and Cdc25B has been observed in a variety of tumor cells including breast cancer [3], colon cancer [4,5], non-Hodgkin's lymphoma [6], prostate cancer [7], pancreatic ductal adenocarcinoma [8], and lung cancer [9,10]. Recent studies have also shown the involvement of Cdc25A in the adhesion-dependent proliferation of acute myeloid leukaemia (AML) cells [11]. Further evidence for the oncogenic property of Cdc25 phosphatases was provided by the pharmacological studies in which the treatment of Cdc25 phosphatase inhibitors retarded the growth of the cancer cell lines expressing a high level of Cdc25 phosphatases [12]. It is likely that the overexpression of either Cdc25A or Cdc25B

* Corresponding author. Tel.: +82 2 3408 3766; fax: +82 2 3408 3334.
** Corresponding author. Tel.: +82 2 875 4887; fax: +82 2 889 1568.
E-mail addresses: sangyoub@snu.ac.kr (S. Lee), hspark@sejong.ac.kr (H. Park).
[1] These authors contributed equally to this work.

1093-3263/$ – see front matter
doi:10.1016/j.jmgm.2008.02.002

leads to the promotion of cell cycle progression in cancer cells although a simultaneous overexpression of both homologues was also observed in more aggressive cancers [13]. Thus, the inhibition of the Cdc25 phosphatases may represent a novel therapeutic approach for the development of anticancer therapeutics although more details about the involvement of Cdc25A and Cdc25B overexpression in tumorigenesis remain to be clarified.

Structural investigations of Cdc25 phosphatases have lagged behind the mechanistic and pharmacological studies. So far two X-ray crystal structures of the catalytic domains of Cdc25A and Cdc25B have been reported in their ligand-free forms only [14,15]. The lack of structural information about the nature of the interactions between Cdc25 phosphatases and small molecule inhibitors has made it a difficult task to discover good lead compounds for anticancer drugs. Nonetheless, a number of effective inhibitors of Cdc25 phosphatases have been discovered with structural diversity as recently reviewed in a comprehensive manner [16–18]. Most of the Cdc25 inhibitors reported in the literature have stemmed from either the isolation of new scaffolds by high throughput screening [19] or the generation of the improved derivatives of pre-existing inhibitor scaffolds [20–24]. Vitamin K_3 (2-methyl-1,4-naphthoquinone) and related compounds are one of the most extensively studied Cdc25 phosphatase inhibitors. Among them, NSC 95397 (2,3-bis-[2-hydroxyethylsulfanyl]-[1,4]naphthoquinone) is a potent Cdc25 phosphatase inhibitor with an IC50 value in the nanomolar range and blocks effectively the G_2-to-M transition [25].

Although no structure of Cdc25 phosphatase in complex with an inhibitor has been reported so far, the binding modes of several inhibitors have also been investigated with docking simulations in the active site of Cdc25B to gain structural insight into their inhibitory mechanism [26,27]. Cdc25A has been excluded in these docking analyses, because its active site revealed in the existing X-ray structure is flatter and more exposed to bulk solvent than that of Cdc25B. These molecular modeling studies revealed that a potent inhibitor should reside in the vicinity of the catalytic thiolate ion of Cys473. It was also shown that the electrostatic interactions with the side chains of the two arginine residues around the active site, Arg482 and 544, would also be the significant binding forces stabilizing an inhibitor in the active site of Cdc25B. However, dynamic properties of the interactions between Cdc25 phosphatases and a potent inhibitor in solution have not been investigated so far. More accurate computational modeling under consideration of the motions of macromolecular protein structure and solvent effects is therefore required to address the details on the mechanism for the inhibition of Cdc25 phosphatases.

In the present study, we examine the dynamic properties of Cdc25B in complex with a potent inhibitor NSC 95397 (Fig. 1) in comparison to those of the ligand-free Cdc25B. The starting structure of the enzyme-inhibitor complex was prepared from docking simulation. The characteristic feature that discriminates our docking simulation from those in the previous studies lies in the implementation of an accurate solvation model, which would have the effect of enhancing the accuracy of the calculated binding mode. Based on the solution-phase molecular dynamics (MD) simulations, we aim to identify the significant binding forces that stabilize the enzyme-inhibitor complex in aqueous solution by measuring the time-evolutions of specific interactions between the protein and the inhibitor groups. During the MD study, we also investigate the motional amplitude of the inhibitor in the active site of Cdc25B and the influence of inhibitor binding on the dynamic stability of the overall protein structure. To the best of our knowledge, we report the first example for a successful application of the solution-phase MD simulation of a Cdc25 phosphatase. It will be shown that the comparative MD studies on bound and unbound forms of a Cdc25 phosphatase can provide valuable information for desinging a new potent inhibitor.

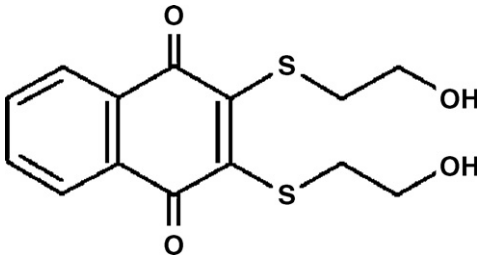

Fig. 1. Molecular structure of NSC 95397.

2. Computational methods

2.1. Docking experiments

We used the AutoDock program [28] to prepare the starting coordinates for MD simulation of Cdc25B in complex with NSC 95397. This program carries out a rapid energy evaluation through precalculated grids of affinity potentials and various search algorithms to find suitable binding conformation for a ligand on a protein receptor. The 3-D coordinates in the crystal structure of Cdc25B in its ligand-free form (PDB code: 1QB0) [15] were selected as the receptor model in the docking simulation. After removing the solvent molecules, hydrogen atoms were added to each protein atom. A special attention was paid to assign the protonation states of the ionizable Asp, Glu, His, and Lys residues. The side chains of Asp and Glu residues were assumed to be neutral if one of their carboxylate oxygens pointed toward a hydrogen-bond accepting group including the backbone aminocarbonyl oxygen at a distance within 3.5 Å, a generally accepted distance limit for a hydrogen bond with moderate strength [29]. Similarly, the lysine side chains were protonated unless the NZ atom was in proximity of a hydrogen-bond donating group. The same procedure was applied to determine the protonation states of ND and NE atoms in His residues. The docking simulation of NSC 95397 onto the active site of Cdc25B was then carried out by applying the Lamarckian genetic algorithm.

In the docking simulation of NSC 95397, we used the empirical scoring function improved with a new solvation

model. The modified scoring function has the following form:

$$\Delta G_{\text{bind}}^{\text{aq}} = W_{\text{vdW}} \sum_{i=1} \sum_{j>i} \left(\frac{A_{ij}}{r_{ij}^{12}} - \frac{B_{ij}}{r_{ij}^{6}} \right) + W_{\text{hbond}} \sum_{i=1} \sum_{j>i} E(t) \left(\frac{C_{ij}}{r_{ij}^{12}} - \frac{D_{ij}}{r_{ij}^{10}} \right) + W_{\text{elec}} \sum_{i=1} \sum_{j>i} \frac{q_i q_j}{\varepsilon(r_{ij}) r_{ij}} + W_{\text{tor}} N_{\text{tor}} + W_{\text{sol}} \sum_{i=1} S_i \left(\text{Occ}_i^{\max} - \sum_{j>i} V_j \, \text{e}^{-r_{ij}^2/2\sigma^2} \right), \quad (1)$$

where W_{vdW}, W_{hbond}, W_{elec}, W_{tor}, and W_{sol} are weighting factors of van der Waals, hydrogen bond, electrostatic interactions, torsional term, and desolvation energy of a ligand, respectively. r_{ij} represents the interatomic distance, and A_{ij}, B_{ij}, C_{ij}, and D_{ij} are related to the depths of energy well and the equilibrium separations between the two atoms. The hydrogen bond term has an additional weighting factor, $E(t)$, representing the angle-dependent directionality. With respect to the distant-dependent dielectric constant, $\varepsilon(r_{ij})$, a sigmoidal function proposed by Mehler and Solmajer was used in computing the interatomic electrostatic interactions between Cdc25B and NSC 95397 [30]. In the entropic term, N_{tor} is the number of sp^3 bonds in the inhibitor. In the desolvation term, S_i and V_i are the solvation parameter and the fragmental volume of atom i [31], respectively, while $\text{Occ}_i^{\max}$ stands for the maximum atomic occupancy. In the calculation of molecular solvation free energy term in Eq. (1), we used the atomic parameters recently developed by Kang et al. [32] because those of the atoms other than carbon were unavailable in the current version of AutoDock. This modification of the solvation free energy term is expected to increase the accuracy in docking simulation, because the conformational dependence of ligand solvation is reflected in the modified scoring function. Then, the most stable configuration of enzyme-inhibitor complex found in docking simulation was selected for the subsequent MD simulation.

2.2. Molecular dynamics simulation

MD simulations of the Cdc25B and its complex with NSC 95397 were carried out with the aid of the SANDER module in AMBER 7 [33] and the force field parameters for proteins reported by Cornell et al. [34]. The derivation of the force filed parameters for NSC 95397 started with the full optimization of its geometry at RHF/6-31G* level of theory with the Gaussian 98 suite of program. Using this energy-minimized structure, each atomic partial charge was calculated at RHF/6-31G* level of theory through the RESP method [35] to be consistent with the standard AMBER force field. As starting structures, we used X-ray structure for ligand-free Cdc25B and its most stable complex with NSC 95397 found in the precedent docking simulation. After adding a sodium ion for charge neutralization, the all-atom models for the unliganded and liganded Cdc25B were immersed in rectangular boxes containing about 8000 TIP3P [36] water molecules. After 200 cycles of energy minimization to remove the bad steric contacts, we equilibrated both systems beginning with 20 ps equilibration dynamics of the solvent molecules at 300 K. The next step involved the equilibration of the solute with a fixed configuration of the solvent molecules consecutively at 10, 50, 100, 150, 200, 250, and 300 K for 10 ps at each temperature. Then, the equilibration dynamics of the entire system was performed at 300 K for 100 ps. Following the equilibration procedure, 2.1 ns MD simulations were carried out with periodic boundary conditions in the NPT ensemble. The temperature and pressure were kept at 300 K and 1 atm using Berendsen temperature coupling [37] and isotropic molecule-based scaling, respectively. The SHAKE algorithm [38], with a tolerance of 10^{-6}, was applied to fix all bond lengths involving hydrogen atom. We used a time step of 1.5 fs and a nonbond-interaction cutoff radius of 12 Å; the trajectory was sampled every 0.3 ps (200-step intervals) for analysis.

3. Results and discussion

Fig. 2 shows the docked pose of NSC 95397 calculated with docking simulations in the active site of Cdc25B. We note that the inhibitor fits the active site pocket with one of its carbonyl groups residing in a close proximity of the catalytic residue Cys473 at a distance around 4 Å. The two terminal hydroxyl groups form hydrogen bonds with the side chain carboxylate group of Glu474 and the backbone –NH group of Arg479. The inhibitor is further stabilized in the active site by the hydrophobic interaction of the phenyl ring with the side chain of Tyr428. The binding mode found in this study differs from those of the previous docking results in which the naphthoquinone moiety of the inhibitors was not accommodated in the active site [25,26]. It is thus apparent that the binding mode of NSC 95397 found in the present study should be more relevant to its inhibitory activity against Cdc25B. This docking result is selected as the starting structure of the successive MD simulation study.

As a check for the stability of protein structure in the course of MD simulations, the time evolutions for the root-mean-square deviation of backbone C_α atoms from the starting structures of production dynamics ($\text{RMSD}_{\text{init}}$) are calculated for the unliganded and liganded Cdc25B. As shown in Fig. 3, the $\text{RMSD}_{\text{init}}$ values remain within 2.5 Å for both bound and unbound simulations, showing a convergent behavior with respect to the simulation time. These results indicate that neither of the two protein structures has undergone a significant conformational change during the entire course of simulation. It is also noteworthy that the $\text{RMSD}_{\text{init}}$ values of Cdc25B-NSC 95397 complex are maintained lower than those of ligand-free CDC25B throughout the whole simulation time. Furthermore, the apoenzyme has a wider range of $\text{RMSD}_{\text{init}}$ values than the enzyme-inhibitor complex. Judging from such differences in dynamic properties of unliganded and liganded Cdc25B, binding of the inhibitor seems to decrease the conformational flexibility of Cdc25B.

As can be seen in Fig. 3, the $\text{RMSD}_{\text{init}}$ values of NSC 95397 remain lower than those of Cdc25B C_α atoms in the former

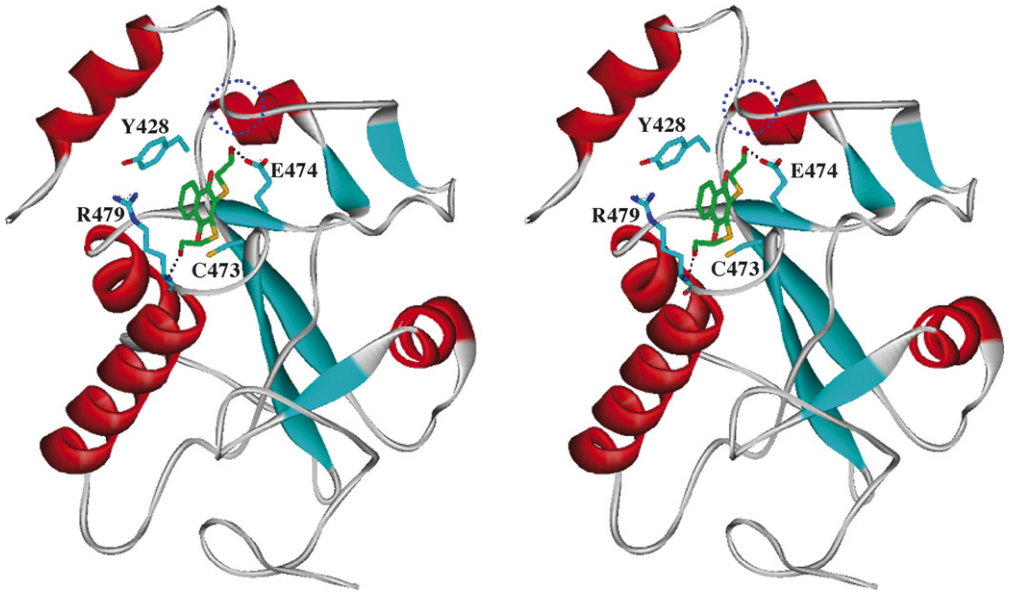

Fig. 2. Stereo view of the binding mode of NSC 95397 in the active site of Cdc25B. Carbon atoms of Cdc25B and NSC 95397 are indicated in cyan and green, respectively. Each dotted line indicates a hydrogen bond. Included in blue circle is the part of the flexible loop (residues 530–532) that exhibits a large change in motional amplitude upon binding of the inhibitor.

stage of the bound simulation, indicating that the movement of the inhibitor should be insignificant within the active site as compared to the conformational changes of the protein. However, the $RMSD_{init}$ values of the inhibitor increase sharply around the simulation time between 1.1 and 1.2 ns, and are maintained comparable to those of the protein. This may be due apparently to a positional shift of the inhibitor to a substantial extent during the stabilization in the active site. Thus, MD simulations of the Cdc25B-NSC 95397 complex in aqueous solution provide more information pertinent to the inhibition mechanism than the precedent docking simulations.

To estimate the changes in dynamic flexibility of the regions of protein structure due to the inhibitor binding, *B*-factors for the C_α atoms (B_i) were calculated using the following relation:

$$B_i = \tfrac{8}{3}\pi^2 \langle \Delta r_i \rangle^2 \quad (2)$$

where $\langle \Delta r_i \rangle$ is the root-mean-square atomic fluctuation of the C_α atom of residue *i*. As shown in Fig. 4, binding of the inhibitor seems to cause the overall decrease in B_i values of Cdc25B, which is indicative of an increase in conformational rigidity of the protein. However, only a few residues of Cdc25B show a significant change in the calculated *B*-factor in the presence of the inhibitor NSC 95397. The calculated B_i values for apoenzyme show a major peak in the region of residues 530–532 that reside near the active site and are the start of the C-terminal region [15]. Judging from the high B_i values, these residues seem to play an important role in the enzymatic

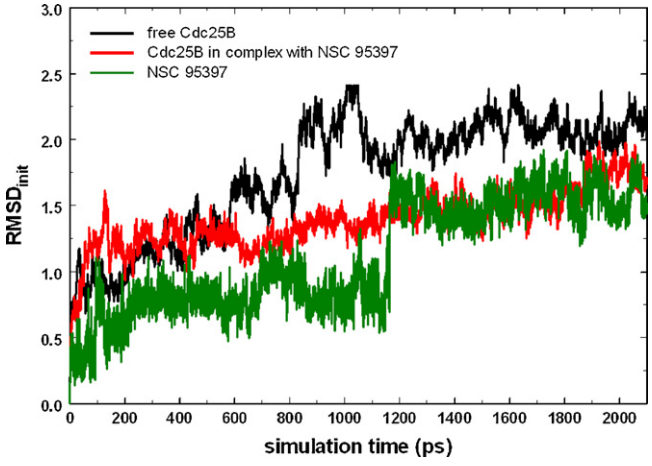

Fig. 3. Time dependences of the root-mean-square deviation of backbone C_α atoms from the starting structure of production dynamics ($RMSD_{init}$) for free Cdc25B (black) and Cdc25B-NSC 95397 complex (red). The green line indicates $RMSD_{init}$ values for all heavy atoms of NSC 95397.

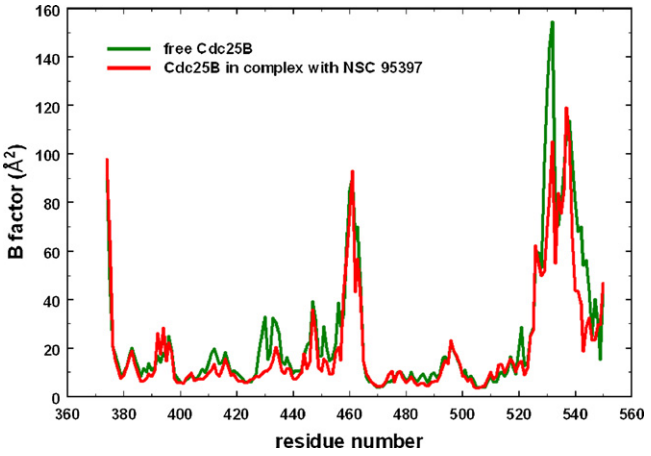

Fig. 4. *B*-factors of the C_α atoms for ligand-free Cdc25B (green) and Cdc25B-NSC 95397 complex (red). Each *B*-factor value is averaged over 1.1 ns time frame from 1.0 to 2.1 ns.

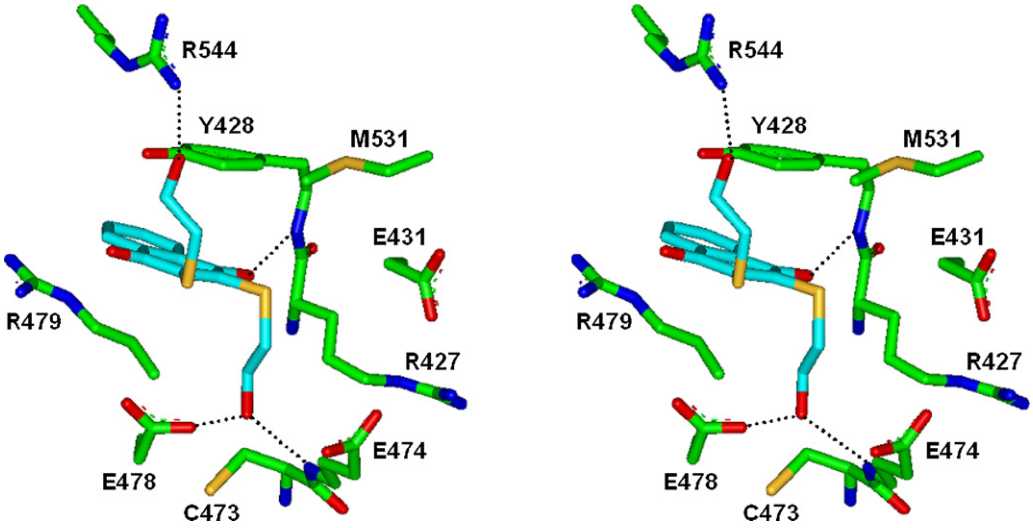

Fig. 5. Stereoview of the representative MD trajectory snapshot of the Cdc25B-NSC 95397 complex. Carbon atoms of the protein and the ligand are indicated in green and cyan, respectively. Each dotted line indicates a hydrogen bond.

function of Cdc25B through a high-amplitude motion. However, binding of the inhibitor reduces the B_i values of the flexible residues by more than 50 Å^2. This implies that such a high-amplitude motion of the flexible residues should be damped out upon binding of the inhibitor in the active site, which may be an explanation for the inhibitory activity of NSC 95397 against Cdc25 phosphatases.

Shown in Fig. 5 is the representative MD trajectory snapshot of the Cdc25B-NSC 95397 complex. We note that one of the hydroxyl groups of the inhibitor receives and donates a hydrogen bond at the bottom of the active site from the backbone amidic nitrogen of Glu474 and to the side chain of Glu478, respectively. The other hydroxyl group of the inhibitor also forms a hydrogen bond with the side chain of Arg544 at the entrance of the catalytic site. The fourth hydrogen bond is established between one of the carbonyl oxygens of the inhibitor and the backbone amide group of Tyr428. Besides the multiple hydrogen bonds, the hydrophobic interactions of the inhibitor with the side chains of Tyr428 and Met531 are observed and also likely to be involved in the stabilization of the inhibitor in the active site of Cdc25B. Judging from a close proximity of Met531 to NSC 95397, the aforementioned decrease in motional amplitude of the flexible residues 530–532 in the presence of the inhibitor may be attributed to the hydrophobic interaction of Met531 with the inhibitor.

To estimate the dynamic stabilities of the hydrogen bonds stabilizing the inhibitor in the active site of Cdc25B, the time evolutions of the associated interatomic distances were calculated and the results of which are shown in Fig. 6. We note that a stable hydrogen bond is established around 1.1 ns between the side chain carboxylate group of Glu478 and the hydroxyl group of the inhibitor and maintained throughout the later part the simulation with 99% of residence time. In a similar time region, two additional hydrogen bonds are also formed in moderate strength: one is between the backbone amidic nitrogen of Glu474 and the inhibitor hydroxyl oxygen and the other between the side chain of Arg544 and the second hydroxyl oxygen of the inhibitor. The former and the latter are maintained for 35% and 45% of the later part simulation time, respectively, when the hydrogen bond defining distance of 2.2 Å is used [29]. Such short residence times indicate the less dynamic stabilities of the two hydrogen bonds as compared to that involving Glu478. The formation of the hydrogen bond between the backbone amide group of Tyr428 and one of the inhibitor carbonyl oxygens lags behind: it is established around 1.7 ns and stabilized after 1.9 ns. When the time evolutions of hydrogen bond interactions are compared with those of the $RMSD_{init}$ values of NSC 95397 shown in Fig. 2, it follows immediately that the substantial positional shift of the inhibitor should be associated with its stabilization in the active site through the formations of the hydrogen bonds, especially that between the inhibitor hydroxyl group and the side chain of Glu478. Judging from the importance of this hydrogen bond, one of the hydroxyl groups seems to play a role of anchor for binding of the inhibitor in the active site. The relative instability

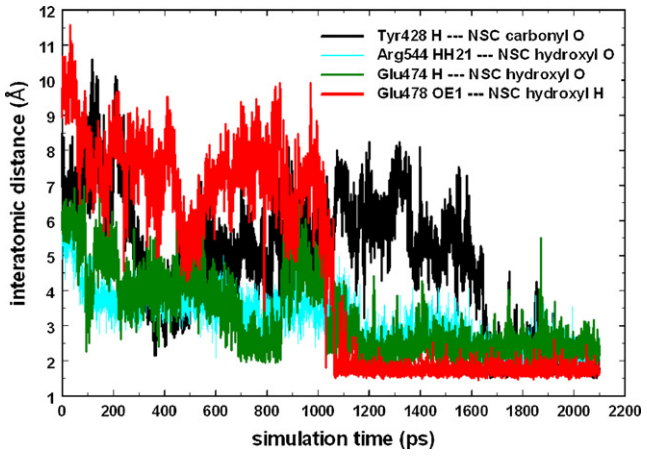

Fig. 6. Time evolutions of the interatomic distances associated with the hydrogen bond interactions of NSC 95397 in the active site of Cdc25B.

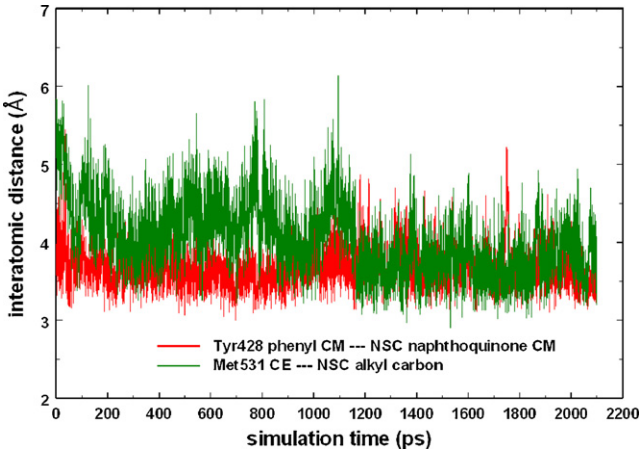

Fig. 7. Time evolutions of the interatomic distances associated with the hydrophobic interactions of NSC 95397 in the active site of Cdc25B.

of the hydrogen bond between Arg544 and the other hydroxyl group indicates that a single hydroxyl group would be sufficient for the inhibitory activity. Indeed, the substitution of methyl moiety for one of the 2-sulfanylethanol groups proved to have little effect on the inhibitory activity against Cdc25B [17].

The stabilities of the hydrophobic interactions between the active site residues of Cdc25B and NSC 95397 may be estimated by examining the time dependences of the associated interatomic distances. As shown in Fig. 7, the distance between the center of mass (CM) of the phenyl ring of Tyr428 and that of the inhibitor 1,4-naphthoquinone ring remains within 4.50 Å for 99% of simulation time with the average of 3.66 Å. Similarly, the separation between one of the alkyl carbons of NSC 95397 and Met531 CE atom falls into 4.50 Å for 84% of simulation time in the enzyme-inhibitor complex. These dynamic stabilities of the interatomic distances indicate that the hydrophobic interactions can serves as a significant binding force stabilizing the inhibitor in the active site of Cdc25B.

4. Conclusions

We have investigated the structural and dynamic properties of ligand-free Cdc25B and its complex with a 1,4-naphthoquinone inhibitor NSC 95397 based on molecular dynamics simulations with explicit solvation. The calculated dynamic properties indicate that the malleability of the residues 530–532 residing around the active site at the start of C-terminal region should be responsible for the catalytic action of Cdc25B. However, the high-amplitude motion of the flexible residues seems to be damped out upon binding of the inhibitor in the active site, due to the hydrophobic interactions with the side chain of Met531. The simulation results also show that at least four hydrogen bonds are involved in the stabilization of the inhibitor in the active site. The most significant dynamic stability is observed for the hydrogen bond between the side chain carboxylate group of Glu478 and one of the hydroxyl groups of the inhibitor. This hydrogen bond seems to play a role of anchor for stabilizing the inhibitor in the active site because the inhibitor undergoes a significant motional shift in such a way to form the hydrogen bond. This may serve as key information for designing new potent Cdc25 phosphatase inhibitors.

Acknowledgments

This work was supported by Grant No. R01-2004-000-10354-0 from the Basic Research Program of the Korea Science & Engineering Foundation. The authors would like to acknowledge the support from Korea Institute of Science and Technology Information (KISTI) under ‘‘The Eighth Strategic Supercomputing Support Program’’ with Dr. Sang Min Lee as the technical supporter. The use of the computing system of the Supercomputing Center is greatly appreciated.

References

[1] K. Kristjansdottir, J. Rudolph, Cdc25 phosphatases and cancer, Chem. Biol. 11 (2004) 1043–1051.
[2] J. Rudolph, Cdc25 phosphatases: structure, specificity, and mechanism, Biochemistry 46 (2007) 3595–3604.
[3] K. Galaktionov, A.K. Lee, J. Eckstein, G. Draetta, J. Meckler, M. Loda, D. Beach, Cdc25 phosphatases as potential human oncogenes, Science 269 (1995) 1575–1577.
[4] S. Hernández, X. Bessa, S. Beá, L. Hernández, A. Nadal, C. Mallofré, J. Muntane, A. Castells, P.L. Fernández, A. Cardesa, E. Campo, Differential expression of Cdc25 cell-cycle-activating phosphatases in human colorectal carcinoma, Lab. Invest. 81 (2001) 465–473.
[5] I. Takemara, H. Yamamoto, M. Sekimoto, M. Ohue, S. Noura, Y. Miyake, T. Matsumoto, T. Aihara, N. Tomita, Y. Tamaki, I. Sakita, N. Kikkawa, N. Matsuura, H. Shiozaki, M. Monden, Overexpression of Cdc25B phosphatase as a novel marker of poor prognosis of human colorectal carcinoma, Cancer Res. 60 (2000) 3043–3050.
[6] S. Hernandez, L. Hernandez, S. Bea, M. Pinyol, I. Nayach, B. Bellosillo, A. Nadal, A. Ferrer, P.L. Fernandez, E. Montserrat, A. Cardesa, E. Cardes, E. Campo, Cdc25A and the splicing variant Cdc25B2, but not Cdc25B1, -B3 or -C, are overexpressed in aggressive human non-Hodgkin's lymphomas, Int. J. Cancer 89 (2000) 148–152.
[7] E.S.W. Ngan, Y. Hashimoto, X.-Q. Ma, M.J. Tsai, S.Y. Tsai, Overexpression of Cdc25B, an androgen receptor coactivator, in prostate cancer, Oncogene 22 (2003) 734–739.
[8] J. Guo, J. Kleeff, J. Li, J. Ding, J. Hammer, Y. Zhao, T. Giese, M. Korc, M. Büchler, H. Friess, Expression and functional significance of Cdc25B in human pancreatic ductal adenocarcinoma, Oncogene 23 (2004) 71–81.
[9] W.G. Wu, Y.H. Fan, B.L. Kemp, G. Walsh, L. Mao, Overexpression of Cdc25A and cdc25B is frequent in primary nonsmall cell lung cancer but is not associated with overexpression of c-myc, Cancer Res. 58 (1998) 4082–4085.
[10] H. Sasaki, H. Yukiue, Y. Kobayashi, M. Tanahashi, S. Moriyama, Y. Nakashima, I. Fukai, M. Kiriyama, Y. Yamakawa, Y. Fujii, Expression of the Cdc25B gene as a prognosis marker in non-small cell lung cancer, Cancer Lett. 173 (2001) 187–192.
[11] A. Fernandez-Vidal, L. Ysebaert, C. Didier, R. Betous, F.D. Toni, N. Prade-Houdellier, C. Demur, M.-O. Contour-Galcéra, G.P. Prévost, B. Ducommun, B. Payrastre, C. Racaud-Sultan, S. Manenti, Cell adhesion regulates Cdc25A expression and proliferation in acute myeloid leukemia, Cancer Res. 66 (2006) 7128–7135.
[12] Y. Nishikawa, B.I. Carr, M. Wang, S. Kar, F. Finn, B. Dowd, Z.B. Zheng, J. Kerns, S. Naganathan, Growth inhibition of hepatoma cells induced by vitamin K and its analogs, J. Biol. Chem. 270 (1995) 28304–28310.
[13] R. Boutros, C. Dozier, B. Ducommun, The when and wheres of Cdc25 phosphatases, Curr. Opin. Cell Biol. 18 (2006) 185–191.
[14] E.B. Fauman, J.P. Cogswell, B. Lovejoy, W.J. Rocque, W. Holmes, V.G. Montana, H. Piwnica-Worms, M.J. Rink, M.A. Saper, Crystal structure of

the catalytic domain of the human cell cycle control phosphatase, Cdc25A, Cell 93 (1998) 617–625.
[15] R.A. Reynolds, A.W. Yem, C.L. Wolfe, M.R. Deibel, C.G. Chidester, K.D. Watenpaugh, Crystal structure of the catalytic subunit of Cdc25B required for G2/M phase transition of the cell cycle, J. Mol. Biol. 293 (1999) 559–568.
[16] M.-O. Contour-Galcéra, A. Sidhu, G. Prévost, D. Bigg, B. Ducommun, What's new on Cdc25 phosphatase inhibitors, Pharmcol. Ther. 115 (2007) 1–12.
[17] S.W. Ham, B.I. Carr, Cell division cycle 25 (Cdc25) phosphatase inhibitors as antitumor agents, Drug Des. Rev. 1 (2004) 123–132.
[18] G.P. Prevost, M.-C. Brezak, F. Goubin, O. Mondesert, M.-O. Galcera, M. Quaranta, F. Alby, O. Lavergne, B. Ducommun, Inhibitors of the Cdc25 phosphatases, Prog. Cell Cycle Res. 5 (2003) 225–234.
[19] J.S. Lazo, D.C. Aslan, E.C. Southwick, K.A. Cooley, A.P. Ducruet, B. Joo, A. Vogt, P. Wipf, Discovery and biological evaluation of a new family of potent inhibitors of the dual specificity protein phosphatase Cdc25, J. Med. Chem. 44 (2001) 4042–4049.
[20] J. Sohn, B. Kiburz, Z. Li, L. Deng, A. Safi, M.C. Pirrung, J. Rudolph, Inhibition of Cdc25 phosphatases by indolyldihydroxyquinones, J. Med. Chem. 46 (2003) 2580–2588.
[21] L. Brault, M. Denancé, E. Banaszak, S.E. Maadidi, E. Battaglia, D. Bagrel, M. Samadi, Synthesis and biological evaluation of dialkylsubstituted maleic anhydrides as novel inhibitors of Cdc25 dual specificity phosphatases, Eur. J. Med. Chem. 42 (2007) 243–247.
[22] W. Huang, J. Li, W. Zhang, Y. Zhou, C. Xie, Y. Luo, Y. Li, J. Wang, J. Li, W. Lu, Synthesis of miltirone analogues as inhibitors of Cdc25 phosphatases, Bioorg. Med. Chem. Lett. 16 (2006) 1905–1908.
[23] M.-P. Brun, E. Braud, D. Angotti, O. Mondésert, M. Quaranta, M. Montes, M. Miteva, N. Gresh, B. Ducommun, C. Garbay, Design, synthesis, and biological evaluation of novel naphthoquinone derivatives with Cdc25 phosphatase inhibitory activity, Bioorg. Med. Chem. 13 (2005) 4871–4879.
[24] M.-O. Contour-Galcéra, O. Lavergne, M.-C. Brezak, B. Ducommun, G. Prévost, Synthesis of small molecule CDC25 phosphatases inhibitors, Bioorg. Med. Chem. Lett. 14 (2004) 5809–5812.
[25] J.S. Lazo, K. Nemoto, K.E. Pestell, K. Cooley, E.C. Southwick, D.A. Mitchell, W. Furey, R. Gussio, D.W. Zaharevitz, B. Joo, P. Wipf, Identification of a potent and selective pharmacophores for Cdc25 dual specificity phosphatase inhibitors, Mol. Pharmacol. 61 (2002) 720–728.
[26] A. Lavecchia, S. Cosconati, V. Limongelli, E. Novellino, Modeling of Cdc25B dual specificity protein phosphatase inhibitors: docking of ligands and enzymatic inhibition mechanism, ChemMedChem 1 (2006) 540–550.
[27] H. Park, B.I. Carr, M. Li, S.W. Ham, Fluorinated NSC as a Cdc25 inhibitor, Bioorg. Med. Chem. Lett. 17 (2007) 2351–2354.
[28] G.M. Morris, D.S. Goodsell, R.S. Halliday, R. Huey, W.E. Hart, R.K. Belew, A.J. Olson, Automated docking using a Lamarckian genetic algorithm and an empirical binding free energy function, J. Comput. Chem. 19 (1998) 1639–1662.
[29] G.A. Jeffrey, An Introduction to Hydrogen Bonding, Oxford University Press, Oxford, 1997.
[30] E.L. Mehler, T. Solmajer, Electrostatic effects in proteins: comparison of dielectric and charge models, Protein Eng. 4 (1991) 903–910.
[31] P.F.W. Stouten, C. Frömmel, H. Nakamura, C. Sander, An effective solvation term based on atomic occupancies for use in protein simulations, Mol. Simul. 10 (1993) 97–120.
[32] H. Kang, H. Choi, H. Park, Prediction of molecular solvation free energy based on the optimization of atomic solvation parameters with genetic algorithm, J. Chem. Inf. Model. 47 (2007) 509–514.
[33] D.A. Case, T.E. Cheatham III, T. Darden, H. Gohlke, R. Luo, K.M. Merz Jr., A. Onufriev, C. Simmerling, B. Wang, R.J. Woods, The Amber biomolecular simulation programs, J. Comput. Chem. 26 (2005) 1668–1688.
[34] W.D. Cornell, P. Cieplak, C.I. Bayly, I.R. Gould, K.M. Merz Jr., D.M. Ferguson, D.C. Spellmeyer, T. Fox, J.W. Caldwell, P.A. Kollman, A second generation force field for the simulation of proteins, nucleic acids, and organic molecules, J. Am. Chem. Soc. 117 (1995) 5179–5197.
[35] C.A. Bayly, P. Cieplak, W.D. Cornell, P.A. Kollman, A well behaved electrostatic potential based method using charge restraints for deriving atomic charges: the RESP model, J. Phys. Chem. 97 (1993) 10269–10280.
[36] W.L. Jorgensen, J. Chandrasekhar, J.D. Madura, R.W. Impey, M.L. Klein, Comparison of simple potential functions for simulating liquid water, J. Chem. Phys. 79 (1983) 926–935.
[37] H.C. Berendsen, J.P.M. Postma, W.F. van Gunsteren, A. DiNola, J.R. Haak, Molecular dynamics with coupling to an external bath, J. Chem. Phys. 81 (1984) 3684–3690.
[38] J.P. Ryckaert, G. Ciccotti, H.C. Berendsen, Numerical integration of the cartesian equations of motion of a system with constraints: molecular dynamics of *n*-alkanes, J. Comput. Phys. 23 (1977) 327–341.